

SUPPORTING INFORMATION

Capturing a Square Planar Gold(III) Complex Inside a Platinum Nanocage: A Combined Experimental and Theoretical Study

Emmanuel Puig,^a Christophe Desmarets,^{*a} Geoffrey Gontard^a, Marie Noelle Rager,^b Andrew L. Cooksy,^c and Hani Amouri,^{*a}

[a] Sorbonne Université-Faculté des Sciences et Ingénierie Campus Pierre et Marie Curie, CNRS, IPCM (UMR 8232), 4 place Jussieu, 75252 Paris cedex 05, France.

[b] Chimie ParisTech, PSL University, NMR Facility, F-75005 Paris, France.

[c] Department of Chemistry, San Diego State U., San Diego CA 921821030, USA

TABLE OF CONTENTS

Figure S1	¹ H NMR spectra in CD ₃ CN /DMSO (4:1) for [Pd ₂ L ₄][OTf] ₄ (1a) in presence of Au(III) guest.
Figure S2	¹ H NMR spectra in CD ₃ CN for a) ligand L and b) the cage complex [Pt ₂ L ₄][OTf] ₄ (1b).
Figure S3	¹ H NMR spectra in CD ₃ CN /DMSO (4:1) for [Pt ₂ L ₄][OTf] ₄ (1b) in presence of Au(III).
Figure S4	¹ H NMR spectra in CD ₃ CN /DMSO (4:1) of the aromatic region for [Pt ₂ L ₄][OTf] ₄ (1b) in presence of Au(III) showing signals due to free cage and complexed cage.
Figure S5	2D NOESY spectrum of [Au(bdt) ₂ ⊂Pt ₂ L ₄][Au(bdt) ₂] ₃ (2) recorded in DMSO.
Table S1	Counterpoise-corrected host-guest interaction energies (kcal/mol).
Table S2	Donor-acceptor interaction energies (kcal/mol) from NBO analysis.
Figure S6	Selected NBO molecular orbitals calculated at the B3LYP/cc-pVDZ,CEP-121G level.

¹H-NMR Studies data for Host Guest Chemistry

For a typical titration experiment, a 7.7 mM solution of cage ($3.87 \cdot 10^{-3}$ mmol) in CD₃CN/DMSO-*d*₆ (4 :1) (0.5 mL) was treated with aliquots of (2.79 mg, $3.87 \cdot 10^{-3}$ mmol) guest followed by an equilibrium time of 5 min prior to the NMR measurement.

Figure S1. ¹H NMR spectra in CD₃CN /DMSO (4:1) for [Pd₂L₄][OTf]₄ (**1a**) in presence of Au(III) guest. a) the cage complex **1a** b) free [*n*-Bu₄N][Au(bdt)₂] guest c) 1 eq. of [*n*-Bu₄N][Au(bdt)₂] d) 1 eq. of [*n*-Bu₄N][Au(bdt)₂] e) excess of [*n*-Bu₄N][Au(bdt)₂] f) free ligand L.

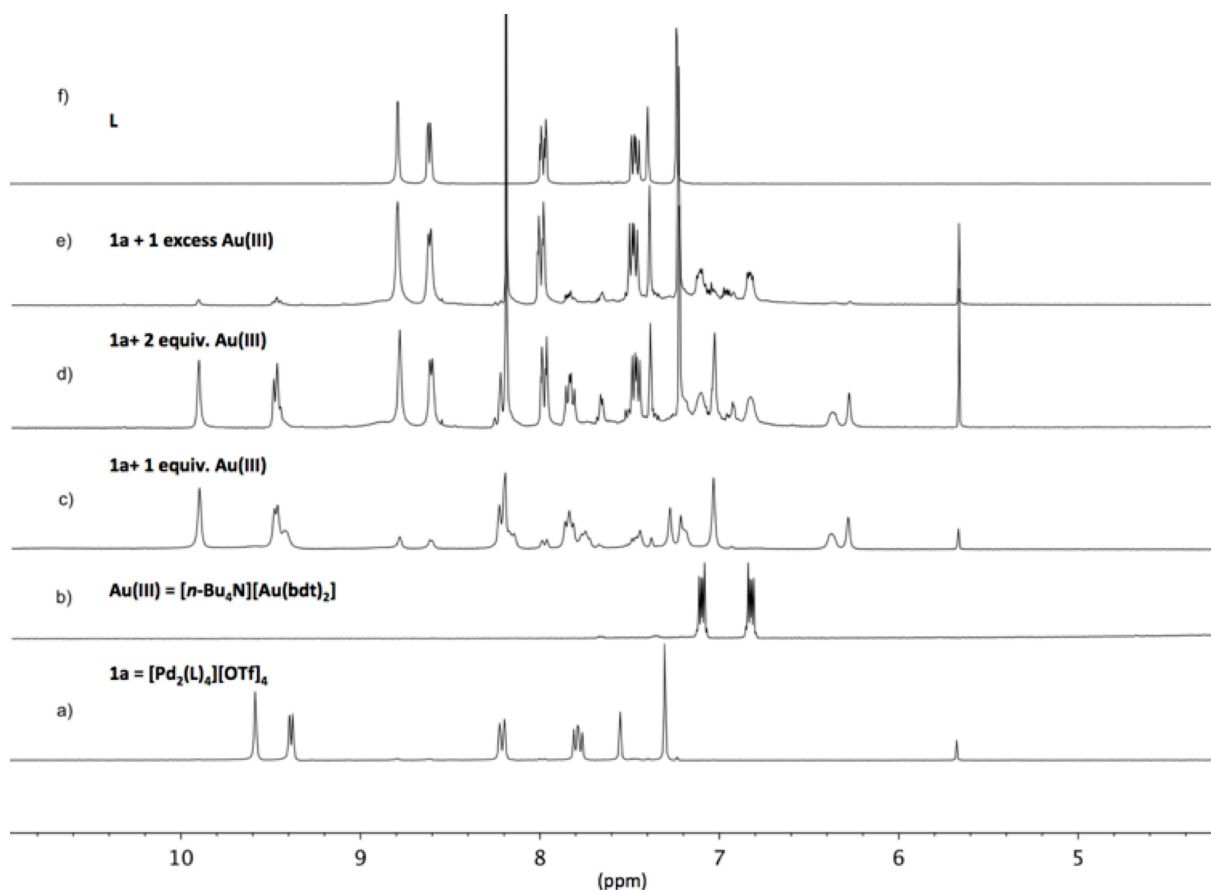


Figure 1 displays the ^1H NMR spectra of compound **1**. The chemical structure of **1** is shown above the spectra. The structure features a central pyridine ring substituted with a 4-methoxyphenyl group and a 2,6-dimethylpyridine-3-yl group. The protons are labeled: H_a (aromatic protons of the pyridine ring), H_b (aromatic protons of the 4-methoxyphenyl group), and H_c (methyl protons of the 2,6-dimethylpyridine-3-yl group).

(a) ^1H NMR spectrum in CDCl_3 . The spectrum shows peaks for H_b (9.1 ppm), H_a (8.6 ppm), aromatic protons (7.8-7.4 ppm), and aliphatic protons (3.9 ppm, 2.1 ppm, 1.2 ppm).

(b) ^1H NMR spectrum in $\text{DMSO}-d_6$. The spectrum shows peaks for H_b (9.1 ppm), H_a (8.6 ppm), aromatic protons (7.8-7.4 ppm), and aliphatic protons (3.9 ppm, 2.1 ppm, 1.2 ppm).

Figure S1 displays four ^1H NMR spectra (a, b, c, d) and their corresponding chemical structures, illustrating the reaction of compound **1b** with Au(III) .

Spectrum (a): Shows the ^1H NMR spectrum of $\text{Au(III)}\text{H}_2$. The structure of $\text{Au(III)}\text{H}_2$ is shown, featuring a gold center coordinated by two thiolate groups and a thiolate ligand. The spectrum shows peaks for H_3 and H_2 in the aromatic region (6.5-7.5 ppm).

Spectrum (b): Shows the ^1H NMR spectrum of compound **1b**. The structure of **1b** is shown, featuring a central carbon atom bonded to two pyridine rings and a methoxy group. The spectrum shows peaks for H_a and H_b in the aromatic region (8.5-9.5 ppm).

Spectrum (c): Shows the ^1H NMR spectrum of **1b** + 1equiv. Au(III) . The spectrum shows peaks for H_e , H_a , H_3 (int), and H_2 (int) in the aromatic region (6.5-9.5 ppm).

Spectrum (d): Shows the ^1H NMR spectrum of **1b** + excess Au(III) . The spectrum shows peaks for H_3 (ext), H_2 (ext), H_3 (int), and H_2 (int) in the aromatic region (6.5-7.5 ppm).

The x-axis represents the chemical shift in ppm, ranging from 0.0 to 10.0.

Figure S4. ^1H NMR spectra in CD_3CN /DMSO (4:1) of the aromatic region for $[\text{Pt}_2\text{L}_4][\text{OTf}]_4$ (**1b**) in presence of sequential additions of Au(III) guest. Signals due to free cage and complexed-cage are visible suggesting a slow exchange is occurring between the Pt-cage and guest Au(III) complex . Ha (star) , Hb (circle) and He (diamond) are denoted in the spectra : Free cage (white symbols); Complexed cage (black symbols).

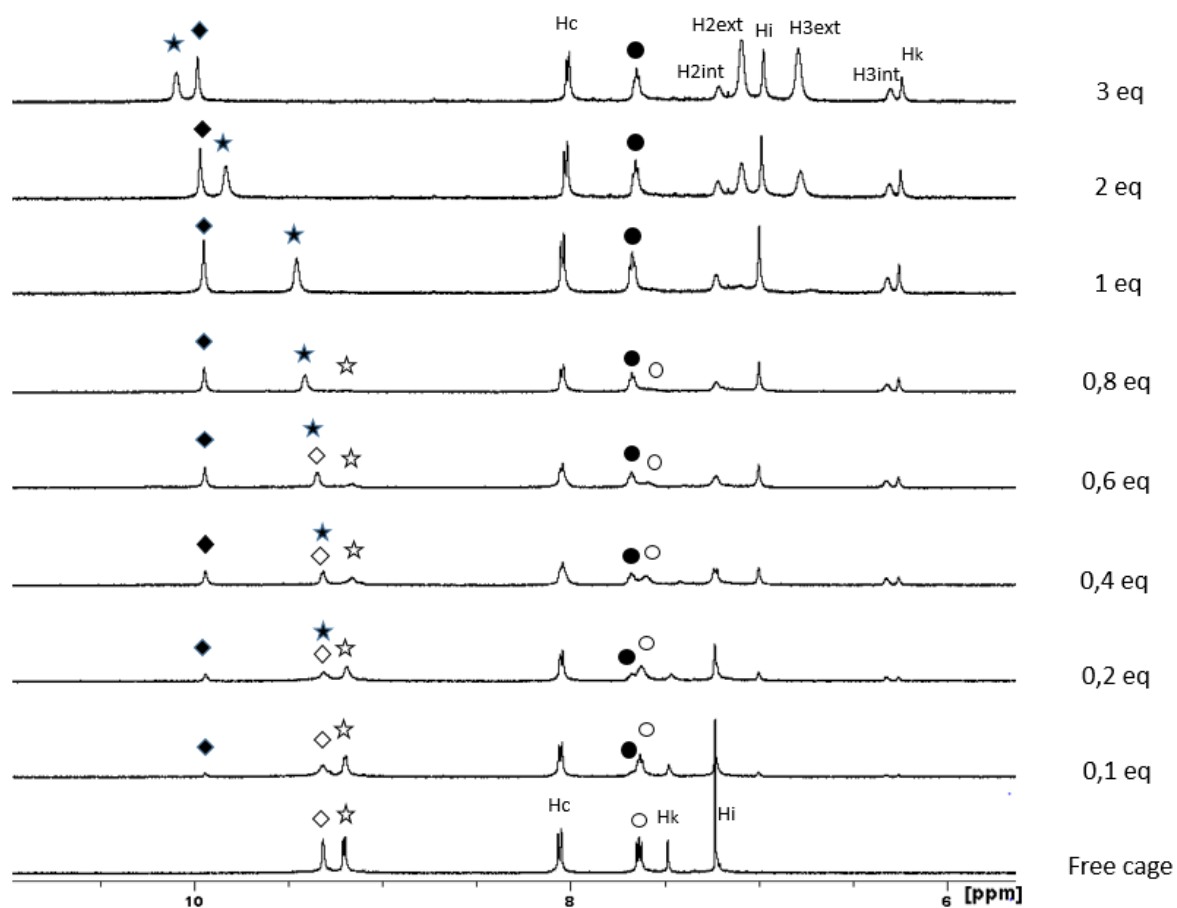
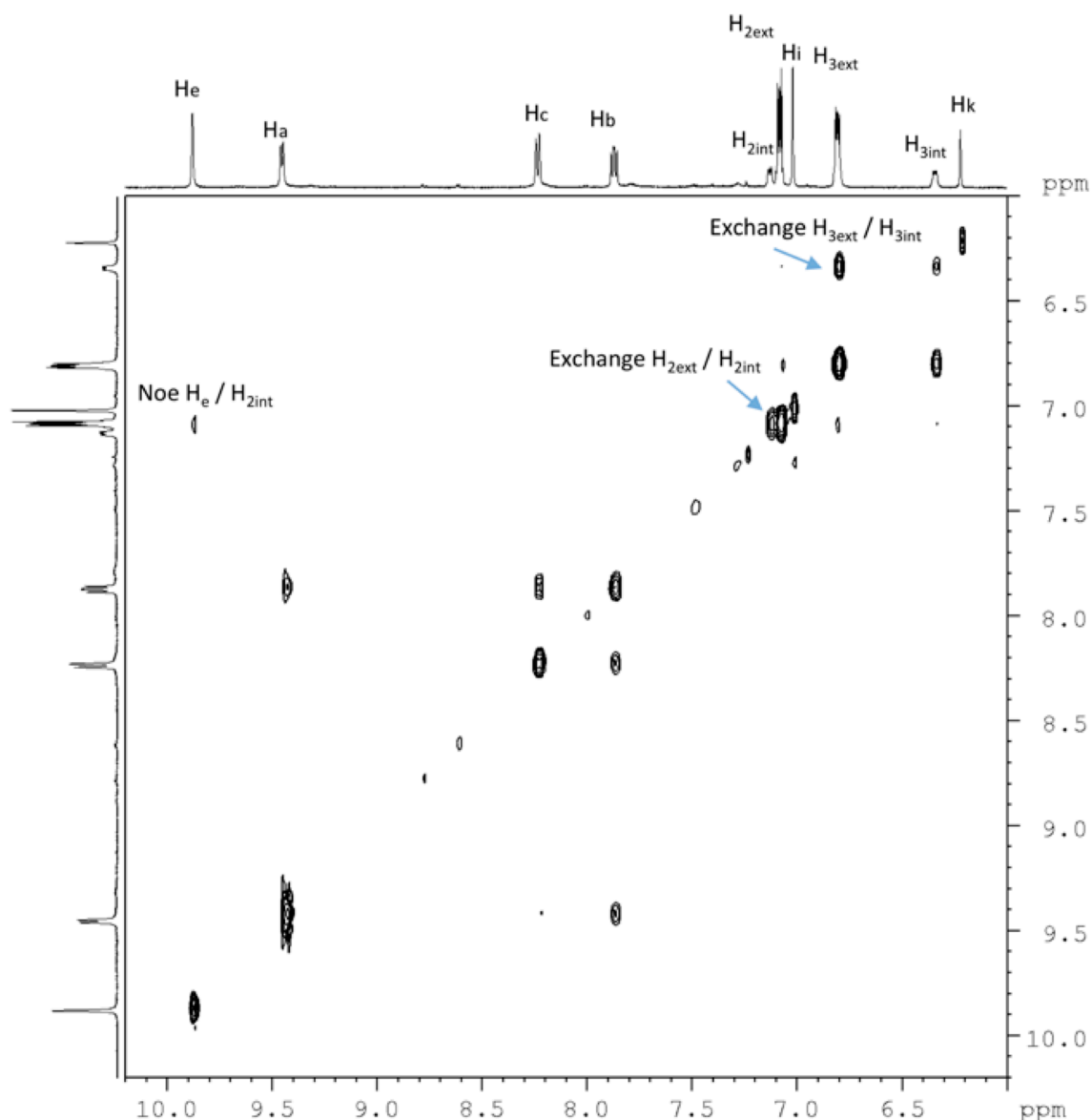


Figure S5. 2 D NOESY spectrum of $[\text{Au}(\text{bdt})_2\text{Cpt}_2\text{L}_4][\text{Au}(\text{bdt})_2]_3$ (**2**) recorded in DMSO.

Computational Details

Properties of the host-guest complex were calculated by density functional theory (DFT), using the popular B3LYP method^{1,2} as well as the more recent M06 method³ and several basis sets for comparison: 3-21G⁴ and cc-pVDZ⁵ for main group atoms, CEP-121G basis and effective core potential⁶ for the metals, and LANL2DZ⁷ for all atoms. The suffix “-D3” added to the method (e.g., “B3LYP-D3”) indicates the inclusion of Grimme's 3-parameter correction⁸ to model dispersion effects. Initial energy and natural bond analysis (NBO)⁹ calculations were carried out using the Gaussian 09 package¹⁰, whereas energy decomposition analysis (EDA)¹¹ was performed using Gamess.¹² In all cases, the fixed X-ray geometry or a truncation of that geometry was used.

The host-guest complexation energies were calculated with counterpoise corrections¹³ in an effort to compensate for basis set superposition error (BSSE). Briefly, BSSE results from the use of a larger number of basis functions to represent the complex than the number of basis functions used for the individual monomers. This discrepancy causes the energy of the complex to be

artificially lower in comparison to the monomers and tends to overestimate binding energies. The counterpoise correction partially addresses this problem by finding the energies of the monomers using the basis set of the entire complex and using these energies to estimate the magnitude of the error.

These energies are predicted to be quite similar among different basis sets and between the B3LYP and M06 methods, which suggests that these basis sets are adequate for calculating the energetics. The interior gold guest is predicted to be more strongly bound than the exterior guest, by 12–18 kcal/mol in the absence of dispersion and by 42–47 kcal/mol when dispersion is included. This seems reasonable, given that the interior guest has more near-atom interactions available and also the possibility of p-stacking interactions between the central methoxyphenyl ring of each arm and the phenyl rings of the guest.

The overall interaction energy of the two guests with the host is greater than the sum of the individual interaction energies, indicating that each guest encourages the host to accept a second guest.

Table S1. Counterpoise-corrected host-guest interaction energies (kcal/mol).

DFT method	basis set	# functions ^a	[host-int] + [ext] ^b	[host-ext] + [int] ^b	[host] + [ext] + [int] ^b
B3LYP	LANL2DZ	1376	-122.4	-140.5	-299.6
B3LYP	cc-pVDZ,CEP-121G	2308	-122.4	-134.9	-294.1
B3LYP-D3	LANL2DZ	1376	-145.2	-192.7	-374.4
B3LYP-D3	3-21G,CEP-121G	1452	-146.2	-189.5	-372.3
B3LYP-D3	cc-pVDZ,CEP-121G	2308	-145.2	-187.1	-368.9
M06-D3	cc-pVDZ,CEP-121G	2308	-142.1	-191.8	-370.2

^a Total number of contracted basis functions for the entire complex. A larger number of basis functions generally implies a better basis set.

^b [host-int] + [ext] represents the energy change upon formation of the entire complex from inserting a gold guest molecule into the complex of Pt₂ metallocage host containing the interior guest; [host-ext] + [int] is DE for inserting the interior guest to form the entire complex; [host] + [ext] + [int] is DE for formation of the entire complex from the host and both guest molecules initially separated.

Most of the interaction energies given in Table S1 are theoretical *gas-phase* binding energies. The binding energy in polar solvent is expected to be lower because the separated ions (particularly the +4 metallocage) will be more strongly stabilized by solvent interactions than the combined +2 complex. However, the effect of the counterions would also have to be incorporated into that calculation, and therefore we have not attempted to model the solution-phase in the present results.

The B3LYP/cc-pVDZ,CEP-121G NBO analysis yields a set of atom-by-atom interaction energies, labeled $E^{(2)}$ calculated by second-order perturbation theory. These values represent individual donor-acceptor interaction energies, including charge-transfer contributions. Summing $E^{(2)}$ values over all of the interactions from atoms of the host to atoms of a guest, we can roughly estimate the total donor-acceptor interaction energy. Those results for this complex are summarized in Table S2. For both the interior and exterior guests, the dominant contribution to these energies

arises from the guest acting as a donor to the organic component of the host cage.

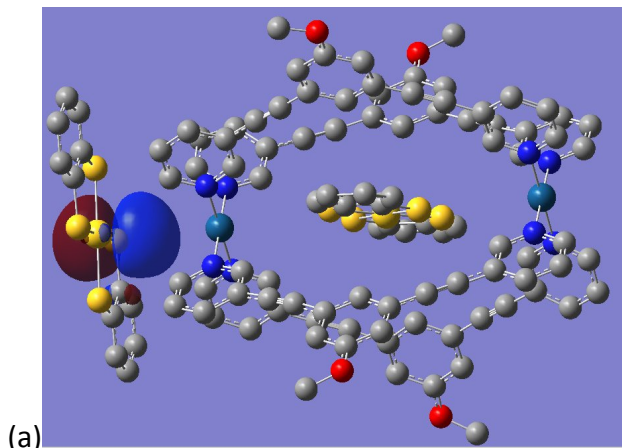
Table S2. Donor-acceptor interaction energies (kcal/mol) from NBO analysis.

donor-acceptor ^a	exterior guest	interior guest
Pt _a - guest	-4.6	-0.2
Pt _b - guest	0	-0.2
cage - guest	-11.3	-2.9
guest - Pt _a	-9.3	-5.9
guest - Pt _b	0	-6.1
guest - cage	-24.6	-36.8
total	-49.8	-52.1

^a Pt_a is the Pt atom adjacent to the exterior guest; Pt_b is opposite the exterior guest; cage consists of the remaining organic component of the host compound.

The possibility of a metal-metal host-guest interaction exists for this complex, but the Pt atoms appear to be too distant from the guest molecules to account for more than about a quarter of the total interaction energy. Looking specifically for Pt-Au interactions, we find that in the case of the exterior guest, most of the energy contribution involving the neighboring Pt atom is ascribed to direct Pt-Au interaction, whereas for the interior guest the Pt atoms interact roughly equally with the Au atom and with the associated S atoms. In either case, however, Pt-Au bonding appears to be a relatively small contribution to the stabilization of these guests. Instead, most of the donor-acceptor stabilization is provided by the nearest-neighbour interactions, especially the electropositive hydrogen atoms on the host aryl groups as the acceptors and the guest sulfur atoms and aryl carbons as donors.

This is consistent in part with the NBO orbital analysis, which predicts the highest energy occupied MOs to be π -type orbitals on each of the four sulfur atoms of the exterior guest molecule, conjugated into the aryl π -system (Fig. S6a). The next highest energy occupied orbitals are the π -bonding orbitals from the two guest phenyl groups (Fig. S6b), which may also act as donor orbitals. The lowest unoccupied orbitals are Pt d orbitals, but candidate acceptor orbitals at the host appear at slightly higher energy (Fig. S6c).



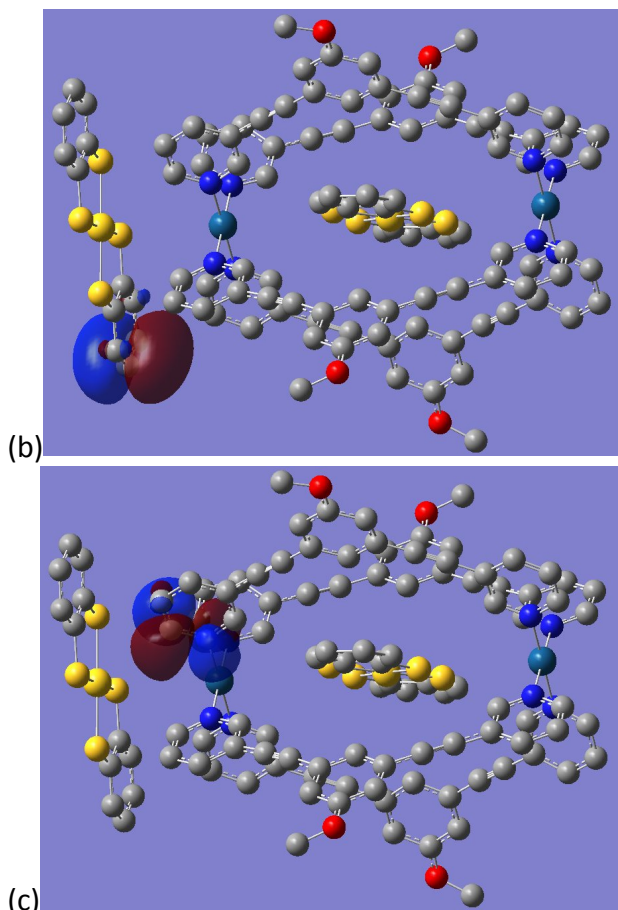


Figure S6. Selected NBO molecular orbitals calculated at the B3LYP/cc-pVDZ,CEP-121G level: (a) the HOMO, a possible donor orbital from the guest S atom; (b) HOMO-4, a possible donor orbital from the guest aryl group; (c) LUMO+8, a possible acceptor orbital.

The importance of S and aryl guest interactions with the host phenyl hydrogens is also consistent with a very crude analysis of the electrostatic interactions between the host and guests based on the approximate formal charges on each atom assigned by the Mulliken method.¹⁴ It should be emphasized that Mulliken charges are extremely sensitive to computational parameters such as basis set, and the energy values we obtain from them are not likely to be accurate. However, it is reasonable to expect that qualitative conclusions about the relative interaction strengths may be drawn from these values. For the exterior guest, average nearest neighbor (guest S)-(host H) distance is 3.21 Å, and the average nearest neighbor (guest C)-(host H) distance is 2.95 Å. For the interior guest, the nearest neighbor average nearest neighbor (guest S)-(host H) distance is 2.87 Å. With partial charges of -0.03e to -0.20e on the electronegative atoms and up to 0.2 on the H atoms, the Coulomb potential energy between the host and guest may account for 40–50 kcal/mol of the total binding energy for the exterior guest and 20–30 kcal/mol for the interior guest.

To more accurately divide the host-guest binding energy into distinct contributions, a thorough energy decomposition analysis (EDA) is desirable. Unfortunately, these are much more resource-intensive calculations than the energy calculations, and a complete EDA of these interactions is prohibitive for a host molecule of this size. Efforts to develop a suitable model for this energy analysis are ongoing. At present, we can only say that both guest molecules appear to be stabilized by a combination of dispersion, donor-acceptor interaction, and electrostatics, each contribution being of magnitude in the tens of kcal/mol. The interior guest appears to be stabilized largely by the dispersion interaction, whereas electrostatic interactions may play a larger

role in stabilizing the exterior guest. Overall, the interior guest is predicted to be more strongly bound to the cage by roughly 40–50 kcal/mol.

References

1. Becke, A. D. Density-Functional Thermochemistry .3. The Role of Exact Exchange. *J. Chem. Phys.* **1993**, *98*, 5648-5652.
2. Lee, C.; Yang, W.; Parr, R. G. Development of the Colle-Salvetti Correlation-Energy Formula into a Functional of the Electron-Density. *Phys. Rev. B* **1988**, *37*, 785-789.
3. Zhao, Y.; Truhlar, D. G. The M06 suite of density functionals for main group thermochemistry, thermochemical kinetics, noncovalent interactions, excited states, and transition elements: two new functionals and systematic testing of four M06-class functionals and 12 other functionals *Theor. Chem. Acc.* **2008**, *120*, 215-241.
4. Binkley, J. S.; Pople, J. A.; Hehre, W. J. Self-Consistent Molecular-Orbital Methods .21. Small Split-Valence Basis-Sets for 1st-Row Elements *J. Am. Chem. Soc.* **1980**, *102*, 939-947.
5. Dunning, J. T. Gaussian-Basis Sets for Use in Correlated Molecular Calculations .1. The Atoms Boron through Neon and Hydrogen. *J. Chem. Phys.* **1989**, *90*, 1007-1023.
6. Stevens, W. J.; Krauss, M.; Basch, H.; Jasien, P. G. Relativistic Compact Effective Potentials and Efficient, Shared-Exponent Basis-Sets for the 3rd-Row, 4th-Row, and 5th-Row Atoms *Can. J. Phys.* **1992**, *70*, 612-630.
7. Hay, P. J.; Wadt, W. R. Ab initio Effective Core Potentials for Molecular Calculations - Potentials for the Transition-Metal Atoms Sc to Hg. *J. Chem. Phys.* **1985**, *82*, 270-283.
8. Schwabe, T.; Grimme, S. Double-hybrid density functionals with long-range dispersion corrections: higher accuracy and extended applicability. *Phys. Chem. Chem. Phys.* **2007**, *9*, 3397-3406.
9. Foster, J. P.; Weinhold, F. Natural hybrid orbitals. *J. Am. Chem. Soc.* **1980**, *102*, 7211-7218.
10. Frisch, M. J.; Trucks, G. W.; Schlegel, H. B.; Scuseria, G. E.; Robb, M. A.; Cheeseman, J. R.; Scalmani, G.; Barone, V.; Mennucci, B.; Petersson, G. A.; Nakatsuji, H.; Caricato, M.; Li, X.; Hratchian, H. P.; Izmaylov, A. F.; Bloino, J.; Zheng, G.; Sonnenberg, J. L.; Hada, M.; Ehara, M.; Toyota, K.; Fukuda, R.; Hasegawa, J.; Ishida, M.; Nakajima, T.; Honda, Y.; Kitao, O.; Nakai, H.; Vreven, T.; Montgomery, J. A., Jr.; Peralta, J. E.; Ogliaro, F.; Bearpark, M.; Heyd, J. J.; Brothers, E.; Kudin, K. N.; Staroverov, V. N.; Kobayashi, R.; Normand, J.; Raghavachari, K.; Rendell, A.; Burant, J. C.; Iyengar, S. S.; Tomasi, J.; Cossi, M.; Rega, N.; Millam, J. M.; Klene, M.; Knox, J. E.; Cross, J. B.; Bakken, V.; Adamo, C.; Jaramillo, J.; Gomperts, R.; Stratmann, R. E.; Yazyev, O.; Austin, A. J.; Cammi, R.; Pomelli, C.; Ochterski, J. W.; Martin, R. L.; Morokuma, K.; Zakrzewski, V. G.; Voth, G. A.; Salvador, P.; Dannenberg, J. J.; Dapprich, S.; Daniels, A. D.; Farkas, Ö.; Foresman, J. B.; Ortiz, J. V.; Cioslowski, J.; Fox, D. J., Gaussian 09, Revision. (Gaussian, Inc., Wallingford, CT, **2009**).
11. Edmiston, C.; Ruedenberg, K. Localized Atomic and Molecular Orbitals *Rev. Mod. Phys.* **1963**, *35*, 457-465.
12. Schmidt, M. W.; Baldridge, K. K.; Boatz, J. R.; Elbert, S. T.; Gordon, M. S.; Jensen, J. H.; Koseki, S.; Matsunaga, N.; Nguyen, K. A.; Su, S.; Windus, T. L.; Dupuis, M.; Montgomery J. A. Jr., General atomic and molecular electronic structure system *J. Comput. Chem.* **1993**, *14*, 1347-1363.
13. Boys, S. F.; Bernardi, F. The calculation of small molecular interactions by the differences of separate total energies. Some procedures with reduced errors *J. Mol. Phys.* **1970**, *19*, 553-566.
14. Montgomery J. A. Jr.; Frisch, M. J.; Ochterski, J. W.; Petersson, G. A. A complete basis set model chemistry. VI. Use of density functional geometries and frequencies. *J. Chem. Phys.* **1999**, *110*, 2822-2827.